*R. Banerjee*
*G. Basu*
*P. Chène*
*S. Roy*

# Aib-based peptide backbone as scaffolds for helical peptide mimics

**Authors' affiliations:**
*Raja Banerjee, Gautam Basu and Siddhartha Roy,* Department of Biophysics, Bose Institute, Calcutta, India.

*Patrick Chène,* Novartis, Basel, Switzerland.

**Correspondence to:**
Dr *Gautam Basu and* Prof. *Siddhartha Roy*
Department of Biophysics
Bose Institute
P-1/12 CIT. Scheme VII M
Calcutta 700 054
India
Tel.: +91-33-3379219
Fax: +91-33-3343886
E-mail: gautam@boseinst.ernet.in;
sidroy@boseinst.ernet.in

**Dates:**
Received 15 January 2002
Revised 9 March 2002
Accepted 10 April 2002

**To cite this article:**
*Raja Banerjee, Gautam Basu, Patrick Chène, & Siddhartha Roy.* Aib-based peptide backbone as scaffolds for helical peptide mimics.
*J. Peptide Res.*, 2002, **60,** 88–94.



ISSN 1397–002X

**Key words:** Aib; hdm2; helix; p53; peptide design; protease resistance

**Abstract:** Helical peptides that can intervene and disrupt therapeutically important protein–protein interactions are attractive drug targets. In order to develop a general strategy for developing such helical peptide mimics, we have studied the effect of incorporating α-amino isobutyric acid (Aib), an amino acid with strong preference for helical backbone, as the sole helix promoter in designed peptides. Specifically, we focus on the hdm2–p53 interaction, which is central to development of many types of cancer. The peptide corresponding to the hdm2 interacting part of p53, helical in bound state but devoid of structure in solution, served as the starting point for peptide design that involved replacement of noninteracting residues by Aib. Incorporation of Aib, while preserving the interacting residues, led to significant increase in helical structure, particularly at the *C*-terminal region as judged by nuclear magnetic resonance and circular dichroism. The interaction with hdm2 was also found to be enhanced. Most interestingly, trypsin cleavage was found to be retarded by several orders of magnitude. We conclude that incorporation of Aib is a feasible strategy to create peptide helical mimics with enhanced receptor binding and lower protease cleavage rate.

**Abbreviations:** CD, circular dichroism; Fmoc, fluorenylmethoxycarbonyl; NMR, nuclear magnetic resonance; RP-HPLC, reverse-phase high-performance liquid chromatography; TFA, trifluoroacetic acid; DMF, di-methyl formamide.

Protein–protein interactions are ubiquitous in all organisms and are vital points where intervention for therapeutic purposes can be targeted (1,2). One method is to take the

traditional route of drug design, and develop small molecules based on virtual and/or real screening. This route has the strength and weaknesses of currently used drug design methodology. Another possible method is to design peptides that mimic the structure of a part of the protein that forms the interface. This strategy is particularly tempting where the binding portion forms a regular secondary structure.

The helix is an important structural element, which has been widely used in nature in protein–protein and protein–nucleic acid interactions. It would thus be desirable to have a general strategy to produce a helical peptide mimic. We wanted to create a general peptide backbone, which is helical and protease resistant, onto which functional groups could be grafted with relative synthetic ease, without changing the overall conformational properties. Among readily available natural and non-natural amino acids, α-amino isobutyric acid (Aib) is an established alanine analog known to strongly favor helical conformations (3–6). Owing to its strong helical preference for the backbone Ramachandran angles, it has been shown to produce helical conformations regardless of other amino acid types present in the peptide. It can also be easily incorporated in standard peptide synthesis protocols (7).

In addition, Aib has the added advantage from the viewpoint of the conformational entropy change that accompanies binding. Since the allowed conformational space for Aib residue is restricted, upon binding, the conformational entropy loss of the Aib residue is expected to be less than the mono-alkylated amino acids that it substitutes (8). Thus, Aib residues should also improve the binding affinity by reducing the loss of conformational entropy upon binding. Finally, since Aib does not belong to the standard amino acid repertoire, peptides containing Aib may be more protease resistant (9), thus overcoming one of the common problems of peptide based drugs, namely, poor stability *in vivo*.

As a test case, we chose the p53–hdm2 interaction (10). p53 is a multidomain protein, which lies at the center of the response to genotoxic stress (11,12). It is an important regulator of cell cycle progression that responds to DNA damage and repair. The *N*-terminal domain 1–42 is responsible for *trans*-activation function and binding with Hdm2, which downregulates the levels of p53 in the normal cell. In some tumor cells, Hdm2 is overexpressed resulting in the inhibition of wild-type p53 present. Thus, inhibition of p53–Hdm2 interaction may be an important intervention strategy for these types of tumor. Although the NMR structural study of the *N*-terminal domain of p53 has shown to be disordered, with little structure (13), the crystal structure of a 15-mer *N*-terminal part of p53-derived peptide (residues 15–29, of which residues 17–29 are ordered in crystal), bound to Hdm2, shows the p53 interaction region to be helical (14). Three residues on one face of the helix, Phe19, Trp23 and Leu26, participate in binding interactions along with some hydrogen bonds.

We chose residues 17–28 of human p53 (ETFSDLWKLLPE), called Np53 hereafter, which includes the three interacting residues, Phe, Trp and Leu, for design of the mimics to inhibit this interaction. The Aib residues were incorporated into the native sequence preserving the core interacting residues. In this article, we report the synthesis, conformation, interaction and protease sensitivities of a designed analog, ETFBDBWKBLBE (where B stands for Aib), called Ep53 hereafter.

## Experimental Procedures

### Peptide design

In order to design a minimalist version of p53 that would retain its binding capacity to Hdm2, possibly with a higher affinity constant, we started with the sequence and the Hdm2-bound conformation of Np53 as shown in Fig. 1. As can be seen from the diagram, Phe3, Trp7 and Leu10 face the same side of the helical-wheel of Hdm2-bound p53 that forms the core binding residues. Asp5 and Lys8 are on the opposite face, poised within interacting (electrostatic) distance. In designing a p53 mimic, we preserved these

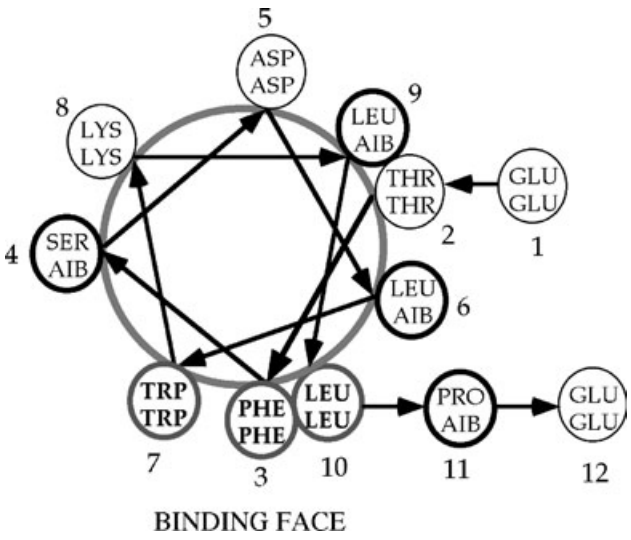


*Figure 1.* Helical wheel representation of the Hdm2 bound conformation of the Np53 peptide and the corresponding sequence of the designed Ep53 peptide.

five residues. In addition, Thr2 was preserved since the *N*-cap position of a helix is often involved in imparting helix stability through capping interactions (15) and Thr2 was found to initiate the helix by H-bond interactions with Asp5. All other residues, except Glu1 and Glu12, were substituted by Aib for its proven ability to promote helix formation in short peptides. All peptides were acetylated at the *N*-termini because it is known to favor helical conformation when present at the *N*-cap position (16). Residue numbering of the peptides used through out this work is given Fig. 1 (Trp23 of human p53 corresponds to Trp7 in our peptides).

#### Peptide synthesis and characterization

The peptides were synthesized on a Fmoc-Glu ($^t$Bu)–Novasyn KA resin (Novabiochem, Switzerland) using standard solid-phase peptide synthesis protocols. Amino acids were either added as Fmoc-Xaa-OpfP esters (Xaa: Leu, Lys (Boc), Trp (Boc), Phe, Glu (OtBu)) or as free Fmoc-Xaa-OH (Xaa: Ser (OtBu), Thr (OtBu), Aib, Asp (OtBu)) with HOBT (N-hydroxy benzotriazole), PyBOP (Benzotriazole-1-yl-oxy-tris-pyrrolidino-phosphorium hexafluoro phosphate) and DIPEA (N,N, diisopropylethylamine) (1 : 1 : 1 : 2). Before the final cleavage from the resin, with TFA–anisole–ethanedithiol–phenol (94 : 2 : 2 : 2, v : v : v : w), *N*-acetylation was achieved with $Ac_2O$ and TEA (1 : 1, tenfold excess with respect to the resin) in DMF. The peptides were finally purified by RP-HPLC using 0–60% $CH_3CN$–$H_2O$ (0.1% TFA) gradient on a $C_{18}$-ODS2 (Waters, MA, USA) column. The major peaks corresponded to the desired peptides as characterized by $^1$H NMR.

#### Circular dichroism measurements

Far-UV circular dichroism spectra were recorded at 8°C and 25°C in a JASCO (Japan) J-700 spectropolarimeter in a 2-mm pathlength thermostated cuvette. The bandwidth was 2 nm and scan speed was 20 nm/min. Samples were prepared in 20 mM phosphate buffer (pH 7.0) with peptide concentrations of approximately 50 μM.

#### Nuclear magnetic resonance spectroscopy

All $^1$H-NMR experiments were performed on a Bruker (Switzerland) DRX 500 MHz spectrometer. Sample were prepared in 20 mM phosphate (pH 7.0) containing 10% $D_2O$ (v : v) with TSP (3-(trimethylsilylpropionic2,2,3,3,d4 acid, sodium salt)) as the internal standard. Water suppression was achieved by using WATERGATE pulse sequence (17) for all experiments. TOCSY (18) and NOESY (19) experiments were performed using standard protocol (20). For structural calculations of Ep53, the αN and NN NOE (Nuclear Ovehaues Effect) crosspeaks were translated into suitable distance upper limits (weak, 3.5 Å; medium, 3.0 Å; strong, 2.5 Å). In addition, the backbone dihedral angles of the Aib residues were restricted ($\phi = -65 \pm 15$; $\psi = -25 \pm 15$). Using these as inputs, 100 structures were generated using the simulated annealing protocol DYANA (21). Based on pairwise rmsd of the structures (residues 4–11 were compared since there were no NMR constraints at the *N*-termini), a cluster analysis yielded families of conformations, discussed later.

#### Hdm2 purification and inhibition assay

The recombinant p53 and GST-hdm2 (1–188), proteins were purified as described earlier (22). The peptides were dissolved in DMSO (dimethyl sulfoxide) and the concentration of the stock solutions was determined spectrophotometrically using an extinction coefficient at 280 nm of 5745 for the Np53 and Ep53 peptides and of 7085 for the AP peptide (23). The peptides were tested for their ability to inhibit the p53–hdm2 interaction in the hdm2 enzyme-linked immunosorbent assay (ELISA) (22) and the $IC_{50}$ values (peptide concentration inhibiting 50% of the interaction between both proteins) were calculated with the GRAFIT (Erithacus Software Ltd., Hovley, Surrey, UK) program.

#### Protease cleavage assay

To approximately 160 μM solutions of Np53 and Ep53 (pH 7.0, 20 mM phosphate buffer), trypsin (1 mg/mL in 1 mM HCl) was added (final peptide–trypsin ratio (w/w) 100 : 1) to initiate digestion at 30°C. After a predesignated time, a fixed amount was taken out, quenched with phenyl-methyl sulfonyl fluoride (final concentration 1 mM) and frozen at –80°C. Trypsin-digested peptide solutions were then subjected to HPLC in $C_{18}$-ODS2 reverse-phase column, using 0–60% $CH_3CN$ gradient in 0.1% TFA as eluent.

## Results and Discussion

### Solution structure of the peptides

Because of reduction of thermal fluctuations, short peptides are known to exhibit their intrinsic helical propensities only at low temperatures. Both Ep53 and Np53 were studied by CD spectroscopy at 25 and 8°C. There was no significant difference in the CD spectra at the two temperatures for either of the peptides. However, in Fig. 2 we show the 8°C spectrum of Np53 and the 25°C spectrum of Ep53 to emphasize that the natural peptide is devoid of any secondary structure even at low temperature, while the Aib analog maintains significant secondary structure even at ambient temperature. As shown in Fig. 2, the Np53 spectrum is dominated by a strong negative minimum below 200 nm, characteristic of random coil conformation. The CD spectrum of Ep53 is dramatically different from that of Np53, characterized by two minima (approximately 225 nm and 203 nm). Although reminiscent of the α-helical CD spectrum (222 nm and 208 nm), the minima are shifted a little from that of a classic α-helix (222 nm and 208 nm) and the intensities are also considerably reduced from a fully-formed helix comprising 12 residues (24). The reduced intensity could arise because of the interference from the Trp residue (25). The presence of four achiral Aib residues could also be responsible for the reduced CD signal due the presence of a minor left-handed helical population. In any event, the CD spectra indicate significant ordered conformation of the helical class in the Ep53 peptide compared with almost random-coil conformation of the Np53 peptide.

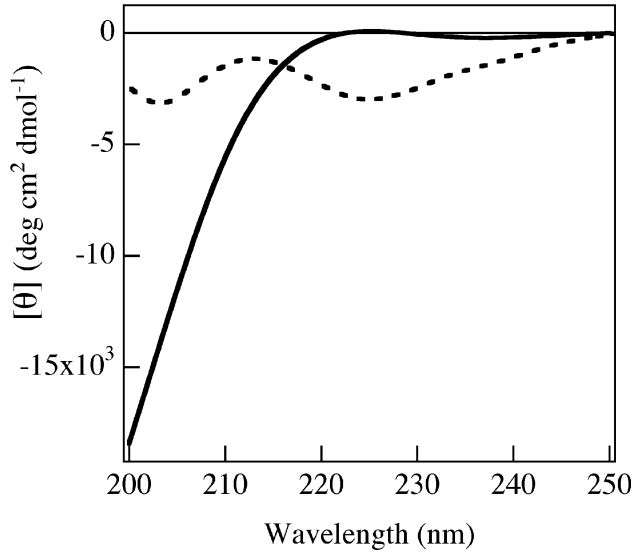


*Figure 2.* Circular dichroism spectra of Np53 (solid line) at 8°C and Ep53 (dashed line) at 25°C in 20 mM phosphate buffer (pH 7.0). The striking difference between the two spectra is attributed to a pronounced helical conformation of Ep53.

Figure 3 shows the difference in $^1$H-NMR chemical shift values of C$^\alpha$H protons from the random coil values (26) — the chemical shift index (CSI). Incorporation of Aib has shifted most C$^\alpha$H protons significantly upfield, suggesting increased preference for a helical structure (27). The upfield shift is most pronounced for Trp7, Lys8 and Leu10 which also show a concomitant lowering of $^3J_{N\alpha}$ values (5.5–4.9, 7.6–5.8 and 7.3–5.8 Hz, respectively) indicating more helical preference. The temperature dependence of the amide protons ($\Delta\delta_{NH}/\Delta T$) can also provide strong supporting

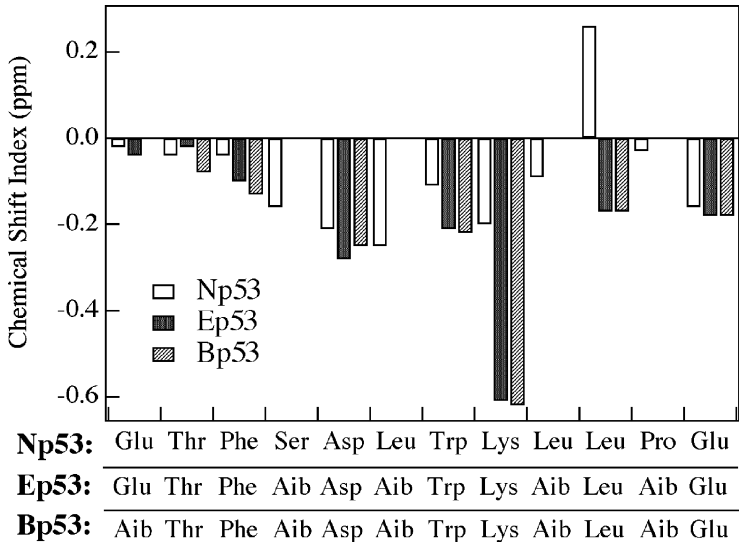


*Figure 3.* Chemical shift index (chemical shift difference of CαH protons from the corresponding random coil values) of Np53, Ep53 and Bp53 peptides at 25°C. Compared with Np53, both Ep53 and Bp53 show a pronounced upfield shift for Trp7, Lys8 and Leu10, indicating induction of a helical backbone upon α-amino isobutyric acid incorporation.

evidence for ordered conformation, arising from intramolecular H-bonds. For Ep53, $\Delta\delta/\Delta T$ values (in p.p.b./K), from Asp (5) to Leu (10) were found to be $= 5$ (except Trp7 for which $\Delta\delta/\Delta T=7$, probably also reflecting ring current effects), while for the rest, the values were $>7$ (data not shown). Clearly, incorporation of Aib has made the peptide more ordered and helical.

The $^1$H-NMR spectra of Np53 and Ep53 showed well-dispersed amide peaks. The $^1$H-NMR spectra were completely assigned using the standard strategy of TOCSY for identifying spin system, followed by sequential assignment from NOESY with different mixing times (250–500 ms). Sequential αN (i,i+1) NOEs were observed for both the peptides at pH 7, 27°C. For peptide Np53, the sequential αN (i,i+1) cross-peaks were more intense compared with the Nα (i,i) cross-peaks, characteristic of extended conformation. Moreover no characteristic nonsequential cross peaks in the αN region were observed. In essence, the NMR data showed Np53 to be in a dominantly disordered conformation, as was already judged by CD. The only $^3J_{N\alpha}$ value that fell in the range of helical backbones corresponded to that of Trp7 ($^3J_{N\alpha}=5.5$ Hz).

The intensity of αN (i,i+1) cross-peaks in Ep53 were comparable or slightly greater than that of Nα (i,i) cross-peaks (for Trp7 the Nα (i,i) cross-peak was more intense than the αN (i,i+1) cross-peak). For a helical backbone, the αN (i,i+1) cross-peaks would have been comparable (or weaker), and for a disordered backbone, the αN (i,i+1) cross-peaks would have been stronger than the Nα (i,i) cross-peaks (27). Therefore, unlike Np53, Ep53 can be considered to be in a partial helical conformation in solution. There were no nonsequential cross-peaks in the Nα region except for a peak between Asp5 C$^\alpha$H and a ring proton of Trp7. Several NN (i,i + 1) cross-peaks were observed: weak (4/5, 8/9 and 10/11), medium (7/8) and strong (6/7). Figure 4 shows several superposed backbone structures of Ep53 derived from NOE distance constraints. The *C*-terminal portion of the peptide is largely ordered and helical whereas the residues in the *N*-terminus are more ill-defined with little NOE constraints. Figure 4 also shows the hdm2-bound conformation of p53 (17–27) peptide (14), which is largely helical. The helical part of the Ep53 peptide is similar to the receptor-bound structure, whereas the *N*-terminal part is disordered.

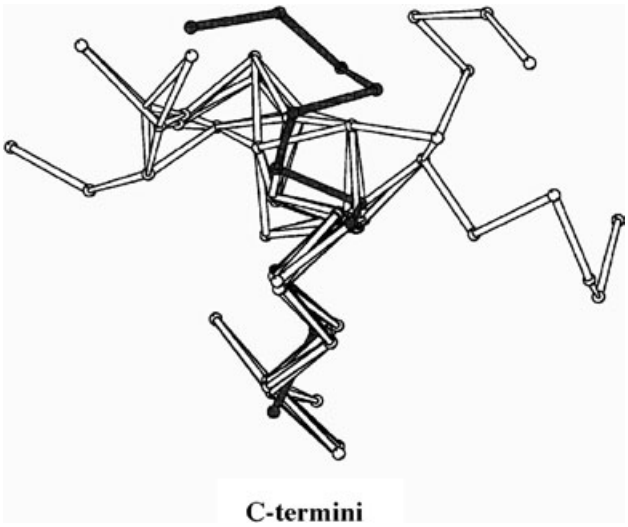


*Figure 4.* A representative conformation cluster ($C^-$ atoms) of Ep53 derived from NOESY distance constraints superimposed with Np53 (shaded dark; residues 1–11) in the hdm2-bound conformation of the p53 peptide.

#### Protease resistance

One of the major problems with peptide-based therapeutic strategies is that they often have a very low biological half-life. In many cases, this is because of initial proteolysis. If peptide mimics are resistant to proteases, they are likely to have a longer biological half-life and consequently their efficacy may improve. Trypsin is a well-known protease, which cleaves the peptide bonds where the *N*-terminal residue is Lys or Arg in the sequence. However, the kinetics of the cleavage also depends on the *C*-terminal amino acid and conformation. Peptides without sufficiently ordered confirmation are much more susceptible to protease activity than others that have ordered conformation. We have determined the trypsin cleavage kinetics for the peptide Np53 and Ep53 using disappearance of the parent RP-HPLC peak upon trypsin digestion. Figure 5 shows the disappearance kinetics upon trypsin cleavage. The Np53 peptide is rapidly degraded and disappears completely within 20 min. In contrast, the Ep53 peptide was found to degrade very slowly and almost 90% of the starting concentration remained even after 3 h. Fitting the data to a first-order kinetic equation yields first-order rate constants of $5.3\times10^{-4}$/min and $1.5\times10^{-1}$/min for Ep53 and Np53, respectively. The almost 300-fold rate difference suggests that multiple Aib substitution can possibly lengthen the biological half-lives of peptide-based agents.

#### Inhibition by the hdm2-binding peptides

The inhibitory activities of Ep53 and Np53 peptides were evaluated in the ELISA hdm2 (22) and their $IC_{50}$ was determined (Table 1). The Ep53 peptide inhibited the p53–hdm2 interaction ($IC_{50}=5.2$ μM) more efficiently than

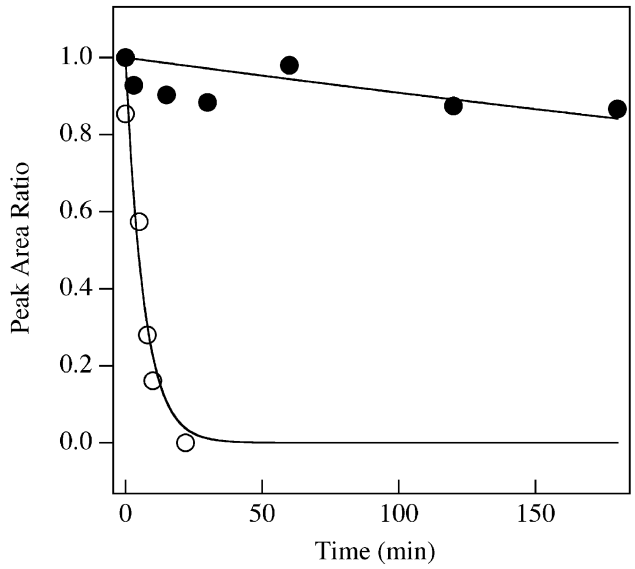


*Figure 5.* Integrated intensities of the parent reverse-phase high-pressure liquid chromatography peaks corresponding to Np53 (filled circles) and Ep53 (open circles) upon trypsin digestion as a function of time. A first-order kinetic analysis yielded rate constants of $5.3\times10^{-4}$/min and $1.5\times10^{-1}$/min for Ep53 and Np53, respectively.

the Np53 peptide ($IC_{50}$=13.5 μM). The $IC_{50}$ values clearly indicate that the more constrained peptide, Ep53, is a better inhibitor of the p53–hdm2 interaction than the natural peptide, Np53, which is more flexible in solution. The $IC_{50}$ values are very promising when compared with the inhibitory activity of a hexamer (TFSDLW) that defines the consensus hdm2-binding site on p53 ($IC_{50}$=700 μM) (28) and comparable to the $IC_{50}$ value (8.7 μM) of a 12-mer wild-type p53-derived peptide, QETFSDLWKLLP (23).

However, inhibition of the hdm2–p53 interaction by Ep53 was about 17-fold less than a 12-mer peptide (MPRFMDY-WEGLN) obtained from an extensive screening with phage display peptide libraries ($IC_{50}$=0.3 μM) (22). To date, the most efficient peptide inhibitor of hdm2–p53 interaction ($IC_{50}$=0.005 μM) is a designed octamer, derived from the 12-mer sequence with extensive side-chain modification and replacement of nonbinding (to hdm2) amino acids by unnatural helicogenic amino acids, including Aib (23). Therefore, although Ep53 showed potent inhibitory activity, for it to be an efficient inhibitor of the hdm2–p53 interaction, side-chain modifications seems inevitable apart from forcing the backbone to adopt a helical conformation mimicking the bound state.

One of our aims was to incorporate as many Aib residues as possible in the noninteracting positions without significantly affecting, or perhaps enhancing,

***Table 1.*** **Inhibition of hdm2–p53 interaction with peptides**

| Peptide | $IC_{50}$ (μM) |
|---|---|
| Np53 | 13.5±0.2 |
| Ep53 | 5.2±0.3 |
| Bp53 | 12.5±0.3 |

interactions with the receptor. A further analog was made where another additional Aib substitution was made at Glu1 (called Bp53). From the CD (not shown) and NMR (CSI values are summarized in Fig. 3) data, the solution conformation of Bp53 was very similar to Ep53. The Bp53 analog showed an $IC_{50}$ of 12.5 μM. In the crystal structure, three side-chains interact exclusively with Mdm2. Thus, even when five (out of eight) expendable side-chains were replaced by Aib, it was possible to maintain native-like affinity. Therefore, it appears that it is a feasible strategy to substitute all or nearly all the expendable amino acids with Aib to enhance protease resistance, while retaining or perhaps even enhancing binding affinity.

## Conclusion

The peptide Ep53 is partly in helical conformation and binds to the receptor with increased affinity (compared with Np53) even though the *N*-terminal portion is still disordered at 25°C. More importantly, the peptide is highly resistant to protease cleavage. In a previous study, it was shown that an octameric peptide, with suitably modified side-chains, could bind to hdm2 with nanomolar affinity (29). Clearly, these side-chains can be grafted on to an Aib-based peptide backbone similar to the ones described in this article to produce highly protease-resistant, soluble peptide mimics which can bind to the receptor with more enhanced binding. Thus, for helical peptides, Aib-based design of peptide mimics appears to be a feasible method for producing lead compounds. Prior to appropriate alteration of the side-chains we are currently designing a peptide that optimizes the placement of Aib residues in Ep53 such that a helical conformation is obtained in isolation along with an enhanced value of $IC_{50}$.

**Acknowledgements:** We thank the Department of Atomic Energy, Government of India, for funding the project. We thank the Bioinformatics Centre for help with computation. We also thank Prof. S. Basak and Jaganmoy Guin for help with the measurement of CD spectra and Barun Majumder for help with the measurement of NMR spectra.

## References


1. Mendelsohn, A.R. & Brent, R. (1999) Protein interaction methods — towards an end game. *Science* **284**, 1948–1950.
2. Marcotte, E.M., Pellegrini, M., Ng, H.L., Rice, D.W., Yeates, T.O. & Eisenberg, D. (1999) Detecting protein function and protein–protein interactions from genome sequences. *Science* **285**, 751–753.
3. Marshall, G.R., Hodgkin, E.E., Langs, D.A., Smith, G.D.J.Z. & Leplawy, M.T. (1990) Factors governing helical preferences of peptides containing multiple α,α-dialkyl amino acids. *Proc. Natl. Acad. Sci. USA* **87**, 487–491.
4. Prasad, B.V. & Balaram, P. (1984) The stereochemistry of peptides containing alpha-aminoisobutyric acid. *CRC Crit Rev. Biochem.* **16**, 307–348.
5. Toniolo, C., Bonora, G.M., Bavoso, A., Benedetti, E., di Blasio, B., Pavone, V. & Pedone, G. (1983) Preferred conformations of peptides containing α,α -disubstituted α-amino acids. *Biopolymers* **22**, 205–215.
6. Basu, G. & Kuki, A. (1992) Conformational preferences of oligopeptides rich in α-aminoisobutyric acid. II. A model for the $3_{10}$/α-helix transition with composition and sequence sensitivity. *Biopolymers* **32**, 61–71.
7. Spencer, J.R., Antonenko, V.V., Delaet, N.G. & Goodman, M. (1992) Comparative study of methods to couple hindered peptides. *Int. J. Pept. Protein Res.* **40**, 282–293.
8. Ratnaparkhi, G.S., Awasthi, S.K., Rani, P., Balaram, P. & Varadarajan, R. (2000) Structural and thermodynamic consequences of introducing alpha-aminoisobutyric acid in the S peptide of ribonuclease S. *Protein Eng.* **13**, 697–702.
9. Nachman, R.J., Isaac, R.E., Coast, G.M. & Holman, G.M. (1997) Aib-containing analogues of the insect kinin neuropeptide family demonstrate resistance to an insect angiotensin-converting enzyme and potent diuretic activity. *Peptides* **18**, 53–57.
10. Finlay, C.A. (1993) The *mdm2* oncogene can overcome wild-type p53 suppression of transformed cell growth. *Mol. Cell. Biol.* **13**, 301–306.
11. Harris, C.C. (1996) Structure and function of the *p53* tumor suppressor gene: Clues for rational cancer therapeutic strategies. *J. Natl Cancer Int.* **88**, 1442–1455.
12. Kubbutat, M.H.G. & Vousden, K.H. (1998) Keeping an old friend under control: regulation of p53 stability. *Mol. Med. Today* **4**, 250–256.
13. Lee, H., Mok, K.H., Muhandiram, R., Park, K.H., Suk, J.E., Kim, D.H., Chang, J., Sung, Y.C., Choi, K.Y. & Han, K.H. (2000) Local structural elements in the mostly unstructured transcriptional activation domain of human p53. *J. Biol. Chem.* **275**, 29426–29432.
14. Kussie, P.H., Gorina, S., Marechal, V., Elenbaas, B., Moreau, J., Levine, A.J. & Pavletich, N.P. (1996) Structure of the *mdm2* oncoprotein bound to the p53 tumor suppressor transactivation domain. *Science* **274**, 948–953.
15. Aurora, R. & Rose, G. (1998) Helix capping. *Protein Sci.* **7**, 21–38.
16. Rohl, C.A., Chakrabartty, A. & Baldwin, R.L. (1996) Helix propagation and N-cap propensities of the amino acids measured in alanine-based peptides in 40 volume per cent trifluoroethanol. *Protein Sci.* **5**, 2623–2637.
17. Piotto, M., Saudek, V. & Sklener, V. (1992) Gradient-tailored excitation for single-quantum NMR spectroscopy of aqueous solutions. *J. Biomol. NMR* **2**, 661–665.
18. Bax, A. & Davis, D.G. (1985) MLEV-17 based two-dimensional homonuclear magnetization transfer spectroscopy. *J. Magn. Reson.* **65**, 355–360.
19. Kumar, A., Ernst, R.R. & Wuthrich, K. (1980) A two-dimensional nuclear Overhauser enhancement (2D NOE) experiment for the elucidation of complete proton-proton cross-relaxation networks in biological macromolecules. *Biochem. Biophys. Res. Commun.* **95**, 1–6.
20. Roberts, G.C. (1993) *NMR of Macromolecules: a Practical Approach*. IRL Press, New York.
21. Guntert, P., Mumenthaler, C. & Wuthrich, K. (1997) Torsion angle dynamics for NMR structure calculation with the new program DYANA. *J. Mol. Biol.* **273**, 283–298.
22. Böttger, V., Böttger, A., Howard, S.F., Picksley, S.M., Chène, P., García-Echeverría, C., Hochkeppel, H.K. & Lane, D.P. (1996) Identification of novel hdm2 binding peptides by phage display. *Oncogene* **13**, 2141–2147.
23. García-Echeverría, C., Chène, P., Blommers, M.J.J. & Furet, P. (2000) Discovery of potent antagonists of the interaction between human double minute 2 and tumour suppressor p53. *J. Med. Chem.* **43**, 3205–3208.
24. Yang, J.T., Wu, C.-S.C. & Martinez, H.M. (1986) Calculation of protein conformation from circular dichroism. *Methods Enzymol.* **130**, 208–269.
25. Chakrabartty, A., Kortemme, T., Padmanabhan, S. & Baldwin, R.L. (1993) Aromatic side-chain contribution to far-ultraviolet circular dichroism of helical peptides and its effect on measurement of helix propensities. *Biochemistry* **32**, 5560–5565.
26. Wishart, D.S., Sykes, B.D. & Richards, F.M. (1992) The chemical shift index: a fast and simple method for the assignment of protein secondary structure through. *NMR Spectrosc. Biochem.* **31**, 1647–1651.
27. Wuthrich, K. (1986) *NMR of Proteins and Nucleic Acids*. John Wiley & Sons, New York.
28. Böttger, V., Böttger, A., Howard, S.F., Picksley, S.M., Chène, P., García-Echeverría, C., Hochkeppel, H.K. & Lane, D.P. (1997) Molecular characterization of the mdm2–p53 interaction. *J. Mol. Biol.* **269**, 744–756.
29. Chène, P., Fuchs, J., Bohn, J., García-Echeverría, C., Furet, P. & Fabbro, D. (2000) A small synthetic peptide, which inhibits the p53–hdm2 interaction, stimulates the p53 pathway in tumour cell lines. *J. Mol. Biol.* **299**, 245–253.